water

MDPI

Article

A Comparison of Design Storms for Urban Drainage System Applications

Rosario Balbastre-Soldevila, Rafael García-Bartual and Ignacio Andrés-Doménech *

Universitat Politècnica de València, Instituto Universitario de Investigación de Ingeniería del Agua y Medio Ambiente (IIAMA), Camí de Vera s/n, 46022 Valencia, Spain; robalsol@cam.upv.es (R.B.-S.); rgarciab@hma.upv.es (R.G.-B.)

* Correspondence: igando@hma.upv.es

Received: 26 February 2019; Accepted: 9 April 2019; Published: 11 April 2019

Abstract: The present research develops a systematic application of a selected family of 11 well-known design storms, all of them obtained from the same rainfall data sample. Some of them are fully consistent with the intensity–duration–frequency (IDF) curves, while others are built according to typical observed patterns in the historical rainfall series. The employed data series consists on a high-resolution rainfall time series in Valencia (Spain), covering the period from 1990 to 2012. The goal of the research is the systematic comparison of these design storms, paying special attention to some relevant quantitative properties, as the maximum rainfall intensity, the total cumulative rainfall depth or the temporal pattern characterising the synthetic storm. For comparison purposes, storm duration was set to 1 hour and return period equal to 25 years in all cases. The comparison is enhanced by using each of the design storms as rainfall input to a calibrated urban hydrology rainfall–runoff model, yielding to a family of hydrographs for a given neighbourhood of the city of Valencia (Spain). The discussion and conclusions derived from the present research refer to both, the comparison between design storms and the comparison of resulting hydrographs after the application of the mentioned rainfall–runoff model. Seven of the tested design storms yielded to similar overall performance, showing negligible differences in practice. Among them, only Average Variability Method (AVM) and Two Parameter Gamma function (G2P) incorporate in their definition a temporal pattern inferred from empirical patterns identified in the historical rainfall data used herein. The remaining four design storms lead to more significant discrepancies attending both to the rainfall itself and to the resulting hydrograph. Such differences are ~8% concerning estimated discharges.

Keywords: design storm; urban drainage; rainfall–runoff

1. Introduction

Design storms, along with intensity–duration–frequency (IDF) curves, are utterly useful tools internationally and widely employed in urban drainage system (UDS) projects and studies. They are used to evaluate the effects of intense rainfall events over a given urban basin, or, most generally, as a tool for urban drainage infrastructures design [1].

Some relevant quantitative properties of a design storm include the value of the maximum or peak rainfall intensity (mm h^{-1}) and the time position it takes place, the total duration of the storm (h), the total cumulative rainfall depth (mm), the centroid of the storm and its temporal pattern.

The design storm corresponds to a given probability level or return period T (years), and in turn conditions the design hyetograph actual magnitude. In most cases, T is related to maximum rainfall intensity, and the same return period is assigned to the maximum peak discharge generated in a given urban catchment. Thus, the design storm and the corresponding estimated hydrograph $Q(t)$

share the same assigned T. Such association is not strictly rigorous, and has been widely discussed in the literature [2,3]. There are several factors explaining this fact. Rainfall intensity process involves fluctuations in both space and time, the storm cells centres frequently experience a significant displacement and the hydrological response of a given rainfall event is dependent on past rainfall and previous state of the catchment. Apart from inherent rainfall complexities, the runoff generating mechanisms are also extremely complex, nonlinear and multivariate in essence [4,5]. From this perspective, it is clear that the use of a single design storm as a unique climatic input to a hydrological system is not very realistic. The use of high-resolution historical records as well as synthetic events derived from stochastic rainfall models can be more accurate and representative, covering a wider range of possible scenarios [6–8]. In fact, these kinds of approaches can be particularly interesting to reproduce a range of possible rainfall situations and conditions, for a hydraulic overall performance assessment of the drainage system [9].

Despite of the above-mentioned aspects, the use of design storms as an efficient engineering tool in urban hydrology studies remains very popular because of its inherent advantages. Among the most remarkable benefits, the following ones should be highlighted. Firstly, it guarantees a uniform level regarding quality and operation standards of the UDS in different urban catchments. Secondly, it reduces and simplifies significantly the hydrologic–hydraulic calculations, when compared with methods employing historical rainfall records or stochastic rainfall models. Such approaches necessarily imply a much higher computational cost, which are not justified in many practical instances of UDS design and operation studies [10–12]. Finally, the circumstances around real urban hydrology engineering applications frequently involve a situation of scarcity of data, being then the design storm approach the most efficient way to tackle the design problem. Moreover, if the design storm is parameterised in a simple form, as some of the design storms described herein, regional approaches including mapping of design storm parameters can be extremely useful in practice for urban drainage design purposes.

Historically, a significant number of methods to obtain design storms have been suggested in the literature, many of them over the decade of the 1970s. Two main groups of design storms can be differentiated: on the one hand, the ones directly inferred from IDF curves, and therefore, those consistent with the rainfall intensity values derived from them. On the other hand, those for which the temporal pattern obeys to other criteria and not just to the information provided by IDF curves. Some authors have highlighted the advantages and drawbacks of these two different approaches [13].

Within the first group, the Chicago Design Storm [14] and its variants, such as the Alternating Block Method [15], are the most representative ones. In order to define this type of design storms, all points in the corresponding IDF curve associated to a given T, or at least, a representative set of points extracted from the aforementioned curved, are used.

Both the Chicago Design Storm and the Alternating Block Method reproduce, in one single theoretical storm, the maximum intensities which were historically found for several durations in different rainfall events. In principle, the resulting design storm has a return period which is, in practice, superior to the one related to the IDF curve from which it derives [14]. Some authors have criticised the choice of this pattern, as it does not actually represent realistically the observed patterns in historical rainfall events [16,17].

Other IDF-based approximations make direct use of only one relevant point of the given intensity–duration curve, suggesting then various geometrical shapes or time patterns, consistent with this previous reading in the intensity–duration curve. Among them, the simplest one is clearly the uniform intensity storm, characterised by a rectangular shape and related to the classic rational method [18]. Other notable storms within this category are the Triangular [19], Sifalda [20], double triangle [21] or Linear/exponential design storms [16].

The rectangular storm exactly reproduces the total cumulative rainfall depth derived from the IDF curve, for a preselected duration. Rainfall intensity is assumed to be constant along the duration of the design hyetograph. The storm proposed by Sifalda [20] divides the above-mentioned total cumulative rainfall depth into three sub-blocks: a first block with increasing rainfall intensities; a second and central one, for which the maximum intensity takes place; and a third one with larger

duration involving decreasing rainfall intensities. The triangular storm [19] is even simpler, and it is built in such a way that the maximum intensity (superior vertex of the triangle) is exactly the double of the average intensity (directly obtained from the IDF curve for a given duration). This design storm represents an extraordinarily simple, yet, sufficiently representative storm for many practical applications [22,23].

The formulation of the Linear /Exponential storm was first suggested by Watt, Chow, Hogg and Lathem [16], after an exhaustive analysis of the maximum rainfall events in Canada. This approach makes use of two analytical trends (i.e., linear and exponential) to represent two stages of the internal rainfall intensity process: one before the rainfall peak occurrence and the other one after the rainfall peak. For early peaking storms, an exponential decay is assumed from the rainfall peak to the end of the storm. In this way, Watt, Chow, Hogg and Lathem [16] develop a 1-h urban design storm for Canada regions, with a two-parameter mathematical model. This strategy provides an important operational advantage, since it considerably facilitates the evaluation of design storms parameters on regional basis, for a range of return periods. The same applies to the G2P design storm [24], which will be introduced later.

With regard to the double triangle storm [21], it can also be obtained solely from readings of the IDF curve. This storm pattern consists of a central triangle overlapping another basic one, in such a way that the resulting storm provides higher peak intensity than the former two storms. Different models in the literature with similar temporal patterns are available [25].

Within the second category, a diversity of design storms can be found in the literature, all of which are formulated on the basis of the typically observed temporal patterns in historical series [13].

The Illinois State Water Survey (ISWS) design storm [26] uses nondimensional patterns, in which the cumulative percent of storm rainfall versus cumulative percent of storm time is represented, after analysis of multiple historical events registered in the state of Illinois (USA). Analogously, the National Resources Conservation Services (NRCS) design storm [27] uses temporal patterns representing the cumulated percentage of rainfall over the daily total versus duration (0–24 h), and therefore, implies a larger time scale than in other previously mentioned design storms.

In Australia, the most extended method is the Average Variability Method (AVM), suggested by Pilgrim and Cordery [28]. This method is based on an exhaustive analysis of the internal structure observed in a family of chosen historical rainfall events. To do so, for a given event, each rainfall interval is ranked according to its rainfall depth. After processing all the available events, each interval or internal period is assigned an average rank. The rainfall intensity for each interval is also calculated in a statistical way. The design storm is then obtained after arranging intervals according to the average rank, and assigning to each one the average percentages of rainfall.

García-Bartual and Andrés-Doménech [24] suggest a simple parameterisation of the storm by using only two parameters, along the lines of Watt et al. [16]. The resulting design storm is analytically defined by a two-parameter gamma function (G2P), and the corresponding parameters are estimated for extreme Mediterranean hydrologic regimes, which are mainly characterised by the occurrence of convective genesis extreme storms. The G2P storm is an early peaking storm with a steep rise until the maximum intensity, followed by gradual rainfall intensity decay until the end of the storm. García-Bartual and Andrés-Doménech [24], compare this G2P design storm with the widely known Alternating Block Method storm.

The aim of the present research is to extend the scope of such comparison, including now a total of 11 popular design storms, all of which derived from the same rainfall data used in García-Bartual and Andrés-Doménech [24]. Additionally, a calibrated rainfall–runoff model is used in this research to incorporate a discussion regarding flow discharges produced by each of the design storms tested herein. This case study consists in an urban catchment located in the city of Valencia (Spain).

2. Rainfall Data

Valencia is located on the eastern coast of Spain, which presents a characteristic Mediterranean semiarid climate—Csa type—according to Köppen–Geiger climate classification [29]. The annual average amounts of rainfall are low (454 mm/year), and they tend to be very unequally distributed

throughout the year. Several mountain ranges run parallel to the coastline, thus forcing humid and warm air coming from the sea to rise into upper atmospheric layers. This phenomenon often occurs during the early autumn, when the sea temperature reaches its maximum. Warm and humid air masses collide with colder upper ones, leading to strong convective cells development, which can generate very high rainfall intensities during short periods. The consequences include frequent, typical, very destructive flash floods that the region experiences almost every year.

The rainfall data used within this research corresponds to the automatic rain gauge located at the headquarters of the Júcar River Basin Water Authority in Valencia (39°28'35'' N 0°21'28'' W elevation: 25 m). This institution manages an automatic hydrological information system which includes 178 automatic rainfall gauges. The rainfall series used in this study is a high-resolution record covering the period from 1990 to 2012, with a time level of aggregation equal to 5 min. Previous studies [30] proved the validity of this data set for similar purposes as the research presented herein. A sample of 73 high-intensity rainfall episodes was extracted from the continuous records [24]. This set of historical rainfall events is also used within this research.

IDF curves are also necessary to build some of the synthetic storms that will be compared herein. They have been estimated using the same 73 aforementioned rainfall episodes. Vaskova [31] used the three parameters potential function [32], successfully representing the local IDF curves in Valencia. Its expression is as follows

$$i\,(t) = \frac{a}{(t+b)^c} \quad (1)$$

where i (mm h^{-1}) is the maximum intensity corresponding to a rainfall duration t (min), while a, b and c are parameters to be estimated for each return period (T). The parameters for the T = 25 years intensity–duration curve (I–D curve) were estimated following the usual procedure for obtaining IDF curves [24]. The resulting values are a = 8198 mm h^{-1}, b = 29.8 min and c = 1.06. The resulting I–D curve is shown in Figure 1. The choice of T = 25 years is in accordance to the requirements established in the local regulations—Municipality of Valencia—for the design of urban drainage hydraulic infrastructures [33].

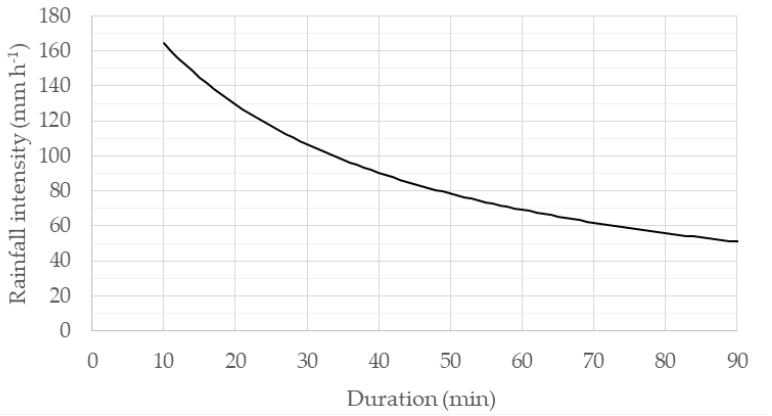

Figure 1. ID curve for T = 25 years (Valencia, Spain).

3. Design Storms

Using the rainfall data described in the previous section, 11 different design storms were derived. As stated before and for comparison purposes, the return period used in all cases was T=25 years. Besides the return period, the storm duration (t_D) and the time level of aggregation (Δt) have been previously set. The storm duration, t_D, was set to one hour, as it is a common storm duration for urban hydrology applications [16]. Indeed, the time of concentration of the Valencian sewer network is less than one hour. On the other hand, maximum intensities in this region are frequently produced by convective cells with average life cycle in small areas varying between 30 and 60 min [34,35]. According to the selected criteria, the maximum expected rainfall intensity in Valencia for T= 25 years and duration of 60 min is 69.27 mm h^{-1}. Concerning the time level of aggregation, and in order to

make use of previous results in the work of García-Bartual and Andrés-Doménech [24], Δt = 10 min was adopted.

The most relevant properties of a given rainstorm are illustrated in Figure 2: maximum rainfall intensity (I_{max}); rainfall depth in each time interval (d_j); total rainfall depth (D); time in which the storm peak intensity is reached (t_P); and first moment or centroid position of the storm event ($\bar{t}$), defined by Equation (2).

$$\bar{t} = \sum_{j=1}^{n} d_j \, (j - 0.5)\Delta t / D \tag{2}$$

where j is the time interval and n the total number of time intervals in which the storm is divided.

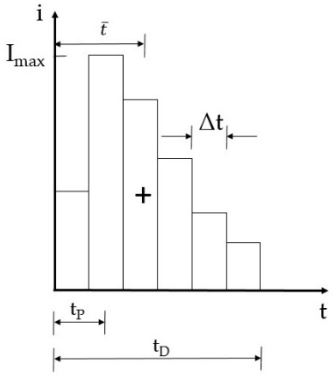

Figure 2. Storm internal characteristics

3.1. Design Storm Description

Table 1 summarises the different design storm methods compared within this research. The two first groups shown in table 1 refer to design storms built directly from IDF curves, while the third one corresponds to hyetographs based on observed rainfall patterns. In each case, the parameters needed to build the design storm are indicated. Further details on these parameters and on the construction procedure can be found in the original reference provided for each method. Nevertheless, some relevant aspects regarding the design storm construction for some of the methods will be remarked herein.

An important consideration to take into account, is the fact that some of the methods were originally proposed for contexts where climatic conditions differ significantly from the one referred herein. Consequently, some of their particularities need to be discussed before applying them to the data used in this research. More specifically, the time scale used in their original formulation differs in some cases from the one used here, making it necessary to adapt their formulation accordingly.

Table 1. Design storm methods.

Classification	Design Storm	Country	Parameters	Reference
Simple geometrical pattern linked to a single point of the IDF curve	(a) Rectangular	United States	T, t_D, I	[36]
	(b) Sifalda	Czechoslovakia	T, t_D, I	[20]
	(c) Double triangle	France	T, t_D, I for each triangle	[21]
	(d) Triangular	United States	T, t_D, I, r	[19]
	(e) Linear/ exponential	Canada	T, t_D, I, r, D, K	[16]
Entire use of the IDF curve for all durations	(f) Alternating blocks	United States	T, t_D, I, Δt	[15]
Standardized profiles of rainfall records	(g) ISWS	United States	t_D, D, quartile distribution	[26,37]
	(h) AVM	Australia	D, storm pattern	[28]
	(i) (j) NRCS	United States	D, distribution type	[27]
	(k) G2P	Spain	φ, i_0	[24]

Parameters: return period, T (years); storm duration, t_D (min); average rainfall intensity, I (mm/h); ratio of storm peak time to storm duration, r; total rainfall depth, D (mm); decay factor, K (5, 6 or 7, depending on region); time interval of aggregation, Δt (min); temporal parameter, φ (min^{-1}); instantaneous peak intensity, i_0 (mm h^{-1}).

For instance, the Illinois State Water Survey (ISWS) design storm temporal pattern was originally established as dependent on the storm duration [37]. Within a later study [38], the ISWS storm temporal pattern adopted is that of the storm duration under 6 h, according to the methodology based on point rainfall data (ISWS-Q1).

In a similar way, the Natural Resources Conservation Service (NRCS) method was conveniently adapted within the framework of this research to obtain a one-hour duration storm event. Therefore, the NRCS is not strictly applied on the basis of its original formulation, but rather modified to match the requirements and initial settings adopted herein. NRCS method considers four time patterns, depending on the region and the storm duration (24 or 6 h) [27]. For the present research purposes, most intense intervals of 1 h duration corresponding to time patterns of the NRCS-6-h and to the NRCS-24-h type II were selected. The resulting design storms will be named NRCS-1 and NRCS-2 respectively.

Regarding the AVM design storm estimation, high temporal resolution rainfall records, described in Section 2, were processed to obtain the average storm pattern required to apply the method, according to Pilgrim and Cordery [28].

With regard to the G2P design storm, it is defined according to Equation (3):

$$i(t) = i_0 f(t) \quad (3)$$

where t is the time elapsed since the beginning of the storm, i_0 is the maximum rainfall intensity of the storm and $f(t)$ is a dimensionless Gamma function with maximum value equal to 1, given by Equation (4):

$$f(t) = \varphi t e^{1-\varphi t} \quad (4)$$

This function $f(t)$ contains the second parameter of the model (φ), and provides a nondimensional time pattern of the design storm. Equation (3) basically tries to describe in a simple analytical way the evolution of rainfall intensity $i(t)$ generated after convective episodes characterised by a rapid rising limb of rainfall intensity until a maximum value is reached, followed by another phase of slower and asymptotic decay in time. The total storm duration is 60 min and the model parameters are φ = 0.0862 min^{-1} and i_0 = 160.8 mm h^{-1} [24]. Following the methodology, the continuous form $i(t)$ allows a discretisation in which rainfall intensities are represented by average values in each of the six intervals of Δt = 10 min.

3.2. Results

Figure 3 shows the resulting design storms, all storms are defined with an internal time level of aggregation equal to 10 min and total duration of 1 hour. For the cases of Sifalda, double triangle, triangular, Linear/exponential and G2P design storms, a dotted line has been added in the figure, showing the original continuous formulation of the design storms. Table 2 summarises the derived

properties of each design storm. Maximum intensities range from 69.3 mm h^{-1} for the rectangular hyetograph to 187.6 mm h^{-1} for the NRCS-2 type storm. The average maximum 10-min intensity is 152.3 mm h^{-1}. Table 2 also shows the relative difference between this average intensity and the peak intensity of each storm. The rectangular, triangular and NRCS-1 hyetographs have maximum intensities below the average value. On the other hand, hyetographs which provide maximum intensities are NRCS-2, double triangle and ISWS-Q1. The design storm with the closest maximum intensity to the average value is the G2P design storm.

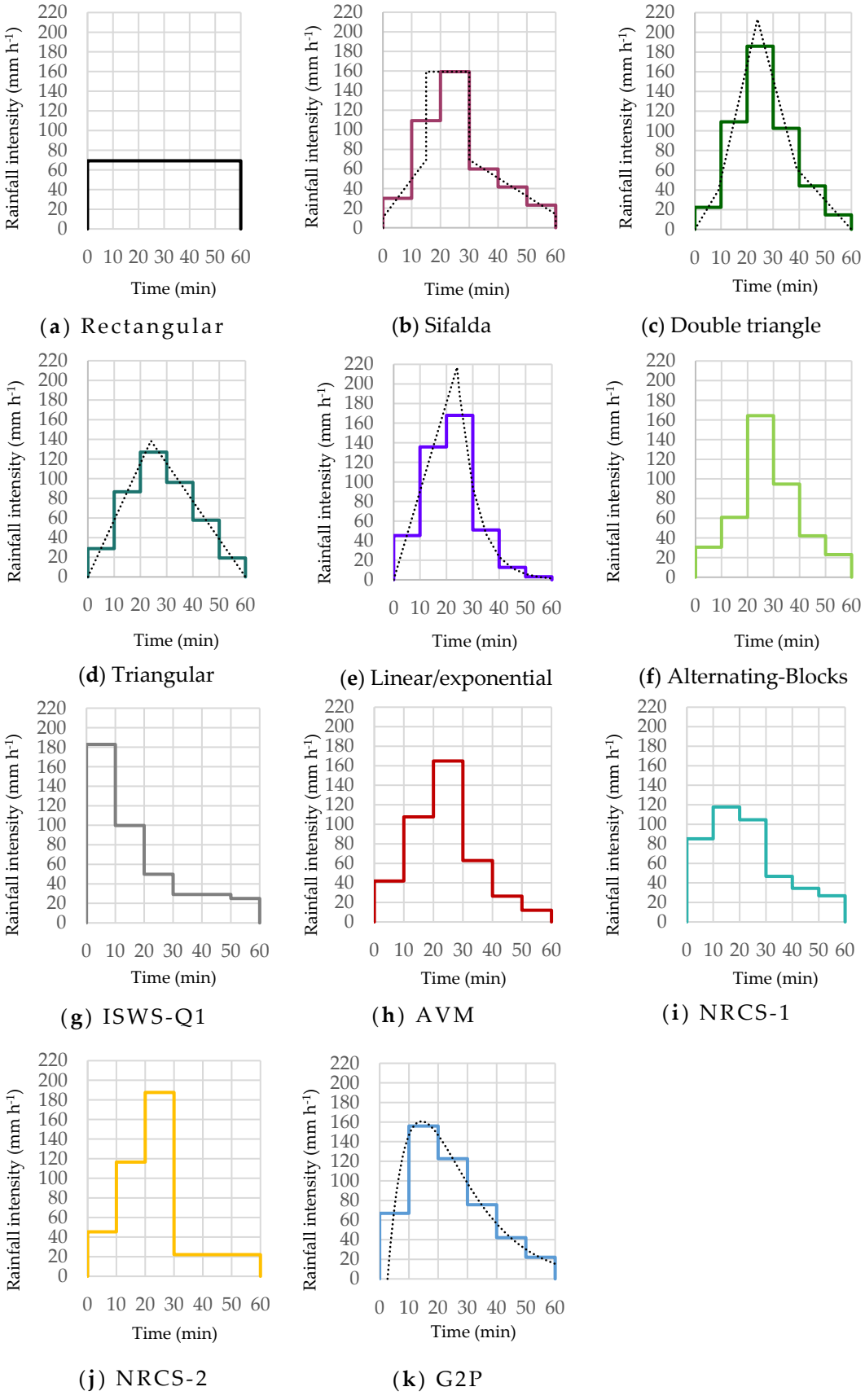

Figure 3. Design storms for Valencia (Spain), T = 25 years. Total duration = 1 hour.

Table 2. Derived properties of the tested design storms.

Design storm	Maximum Intensity I_{max}	Relative Difference ΔI_{max}	Rainfall Depth D	Relative Peak Time t_P/t_D	Relative Centroid $\bar{t}/t_D$
	(mm/h)	(%)	(mm)	(-)	(-)
Rectangular	69.3	−54.7%	69.27	0.50	0.50
Triangular	127.0	−17.0%	69.27	0.40	0.47
Alternating blocks	164.4	7.4%	69.27	0.40	0.47
Sifalda	159.3	4.1%	70.57	0.42	0.43
Double triangle	185.9	21.5%	79.79	0.40	0.45
Linear/exponential	167.9	9.8%	69.27	0.40	0.36
ISWS-Q1	182.9	19.5%	69.27	0.08	0.30
AVM	164.9	7.8%	69.27	0.42	0.40
NRCS-1	117.8	−23.0%	69.27	0.25	0.38
NRCS-2	187.6	22.6%	69.27	0.42	0.39
G2P	156.0	2.0%	80.89	0.20	0.40

Regarding the resulting total cumulative rainfall depths, the highest values are those of Sifalda, double triangle and G2P design storms. For such design storms, the 1-hour intensity reading from the ID curve is not reproduced. These differences in cumulative rainfall depth might be relevant in cases of hydrological applications where the total runoff volumes are important, for instance, urban infrastructures design where the storage volumes play a significant role (i.e., storm tanks or sustainable urban drainage systems).

Storm temporal patterns can be also analysed by comparing the cumulative depths over time (Figure 4).

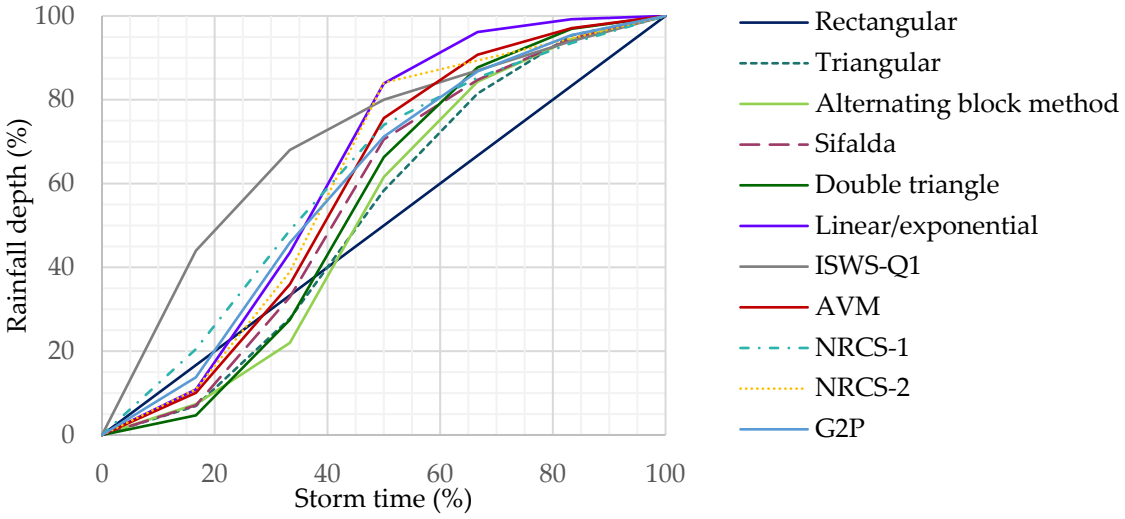

Figure 4. Cumulative rainfall depth (%) curves for the design storms.

As Figure 4 illustrates, almost all patterns follow a typical sigmoidal shape. The beginning and end of the storm correspond to reduced slope intervals, whereas the central region with higher slopes and thus higher rainfall intensities, concentrates a significant portion of the total cumulative depth of the storm. It should be noted, however, that there are two exceptions to this general pattern. First, the rectangular design storm, which obviously follows a straight line in Figure 4. Secondly, the ISWS-Q1 storm, which was also expected to present a different shape, because according to the first quartile distribution, more than 60% of the total cumulative depth occurs during the first 25% (15 min in our case) [37].

Peak time position (t_P) is related to the average slope of the ascending and descending parts of the hyetographs. The earlier the peak occurs, the higher the slope of the rising limb. The centroid position also provides information about the distribution of the cumulative depth over the storm duration. Figure 5 shows the relative peak time position versus the relative centroid position for each design storm. Methods based on IDF curves are represented with dots, while methods based on observed rainfall patterns are represented with squares. It can be seen that almost all design storms present a rising limb until rainfall intensity reaches its maximum value, followed by a longer descending limb. The only two exceptions to this general pattern are the rectangular and ISWS-Q1 hyetographs. As expected, there is a positive correlation ($R^2 = 0.57$) between the two variables shown in Figure 5. Seven design storms (triangular, Alternating Blocks, Sifalda, Linear/exponential, AVM and NRCS-2) present a relative peak time of ~0.40. The rest of the hyetographs present an earlier peak occurrence (with the exception of the rectangular one).

For methods based on internal observed temporal patterns, the storm centroid occurs before the average centroid time for all methods. This means that in relative terms, more rainfall volume before $t = t_P$ is accumulated, when compared to methods directly based on IDF curves. The only exception in this case is the Linear/exponential design storm, which also presents an early centroid position.

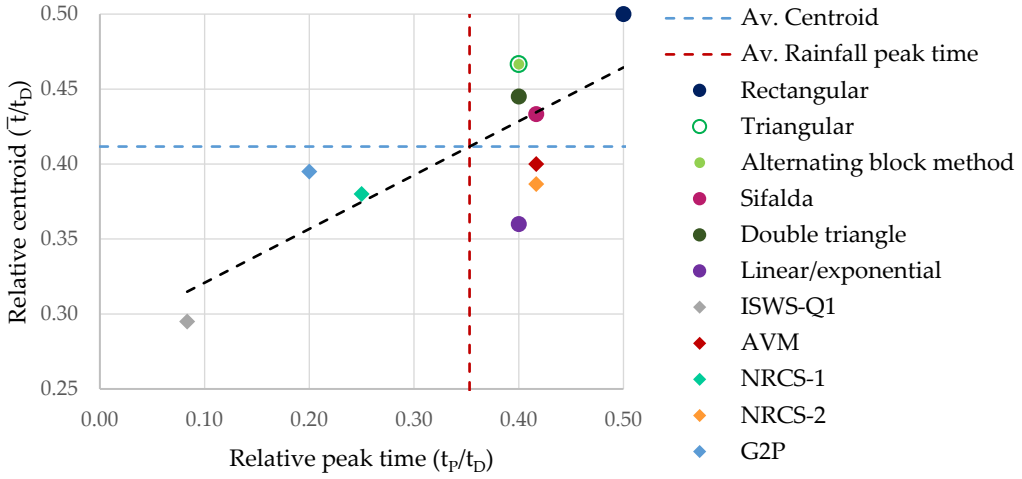

Figure 5. Relative peak time and centroid positon for the design storms.

4. Application to an Urban Drainage Modelling Case Study

Runoff hydrographs can be interpreted as smoothed convolutions of past and current rainfall over the catchment contributing area and along time-dependent hydrological parameters such as time of concentration. Thus, runoff hydrographs characteristics are strongly dependent on rainfall hyetographs inputs. Nevertheless, different authors have reported the filtering effect of the catchment on this convolution [39]. Along the lines of previous work done by Alfieri et al. [40], the main objective in this section is to explore the influence of the above-analysed design storms, after the filtering effect of the rainfall–runoff process in a given catchment. Alfieri et al. [40] used in their research an ideal basin with a linear and time-invariant hydrologic response.

The analysis presented herein is carried out in an instrumented urban catchment located in the city of Valencia (Spain). The sewer network of the city is a combined system, actually resulting from centuries of evolution. Recent studies with the water management service of the city council allowed calibration and validation of a mathematical drainage model of one of the main northern catchments of the city [41]. Figure 6 shows the location and extension of this catchment. It has an extension of 8.1 km^2 and it includes one of the main and most important combined sewer systems of the city. The wastewater treatment plant (WWTP) is located at the south bound of the city. Sewer overflows during storm events spill into the docks.

The urban drainage mathematical model is developed under Infoworks ICM [42]. The model runs the hydrology and hydraulics of the complete urban sewer system. The full Saint–Venant

equations are used to model flows within the sewer network. The implicit Preissmann scheme [43] is used to solve the equations system. Regarding hydrology, the rainfall–runoff transformation is modelled adopting the SCS-CN method, with three different land uses: roads, buildings and green areas. Finally, the surface routing is modelled with a nonlinear reservoir model. The calibration and validation procedures and estimated model parameters can be found in Cabo López [41].

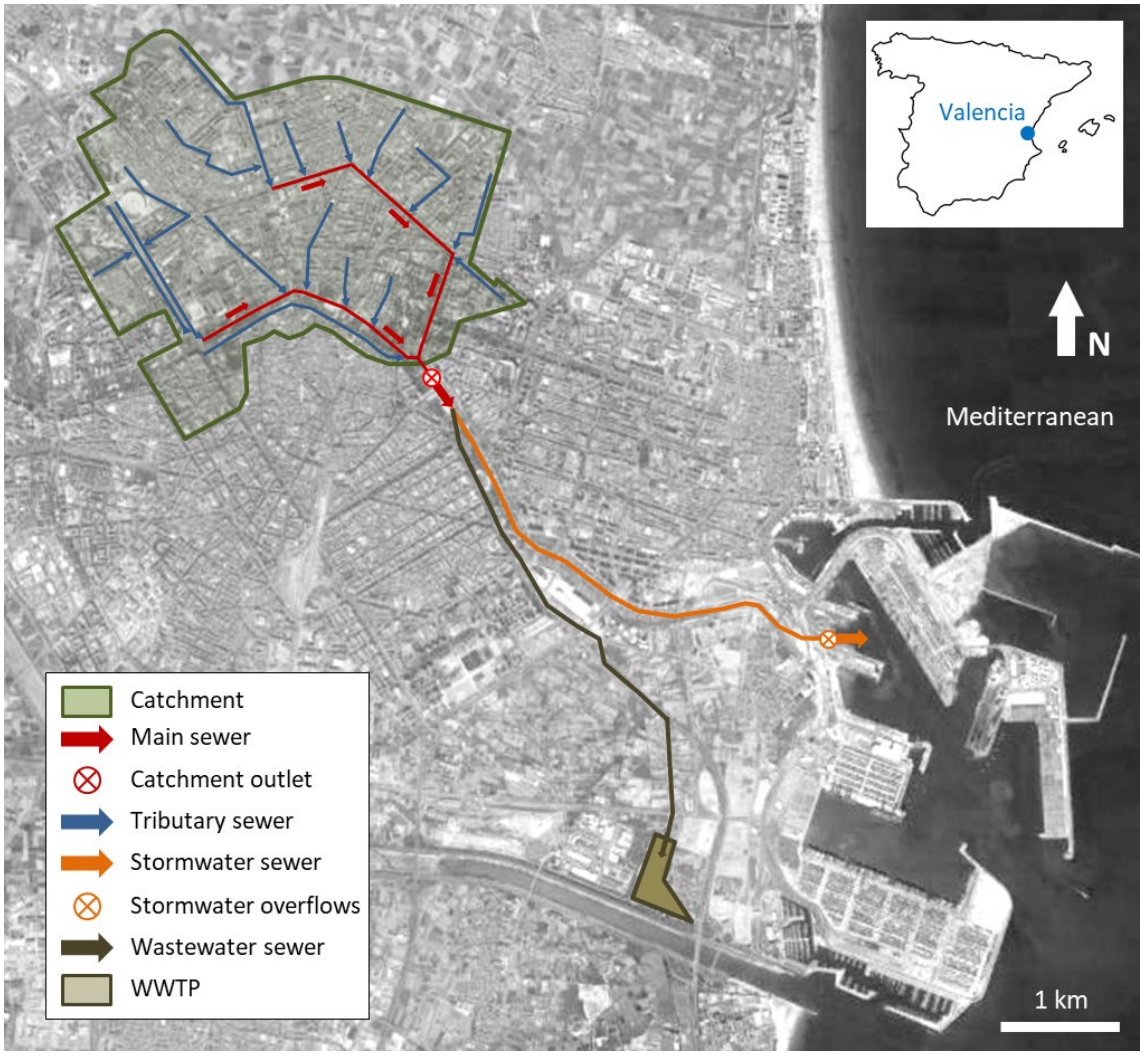

Figure 6. Analysed catchment at the headwaters of the North sewer system of Valencia.

The model is run for the different design storms previously described. For each one of them, runoff hydrographs have been obtained at the outlet of the catchment. Figure 7 represents the resulting hydrographs, and Table 3 summarises the main hydrological descriptors of such runoff hydrographs: peak flow (Q_P), time-to-peak flow (t_{QP}), lag time (t_L) and runoff volume (R). Also, the relative differences of the peak flows with respect to the average Q_P value have been calculated.

Table 3. Comparison of peak flow, characteristic times and volume of the hydrographs resulting from the transformation of each design storm.

	Q_P	ΔQ_P	t_{QP}	t_L	R
	($m^3\ s^{-1}$)	**(%)**	**(min)**	**(min)**	**(hm^3)**
Rectangular	73.4	−9.54%	65	35	0.301
Triangular	80.2	−1.15%	50	26	0.292
Alternating block	82.0	1.06%	46	22	0.291
Sifalda	81.0	−0.17%	42	17	0.298
Double triangle	87.9	8.34%	42	18	0.344
Linear/exponential	85.6	5.50%	39	15	0.290
ISWS-Q1	73.7	−9.17%	30	25	0.294
AVM	83.1	2.42%	42	17	0.291
NRCS-1	75.3	−7.19%	39	24	0.294
NRCS-2	84.8	4.52%	37	12	0.291
G2P	85.5	5.38%	42	30	0.351

As it can be observed in Table 3, double triangle and Linear/exponential produce the largest values of Q_p. The main differences concerning Q_p are found in the hydrographs obtained from the rectangular storm (−9.54 %), ISWS-Q1 storm (−9.17 %) and NRCS-1 storm (−7.19 %), which apparently underestimate maximum peak flow.

In general, there are no significant differences between them, with one expected exception, that is, the hydrograph resulting from the rectangular design storm, which actually ignores the real internal patterns of the storm. Additionally, and as expected too, the corresponding peak discharge occurs at the end of the storm. Concerning time-to-peak, most hydrographs yield to similar results (t_{QP} = 43 ± 7 min). Only two exceptions should be pointed out: the hydrographs after the rectangular design storm (t_{QP} = 35 min) and the ISWS-Q1 design storm (t_{QP} = 30 min). These differences could be relevant in some cases, i.e., storm tanks design.

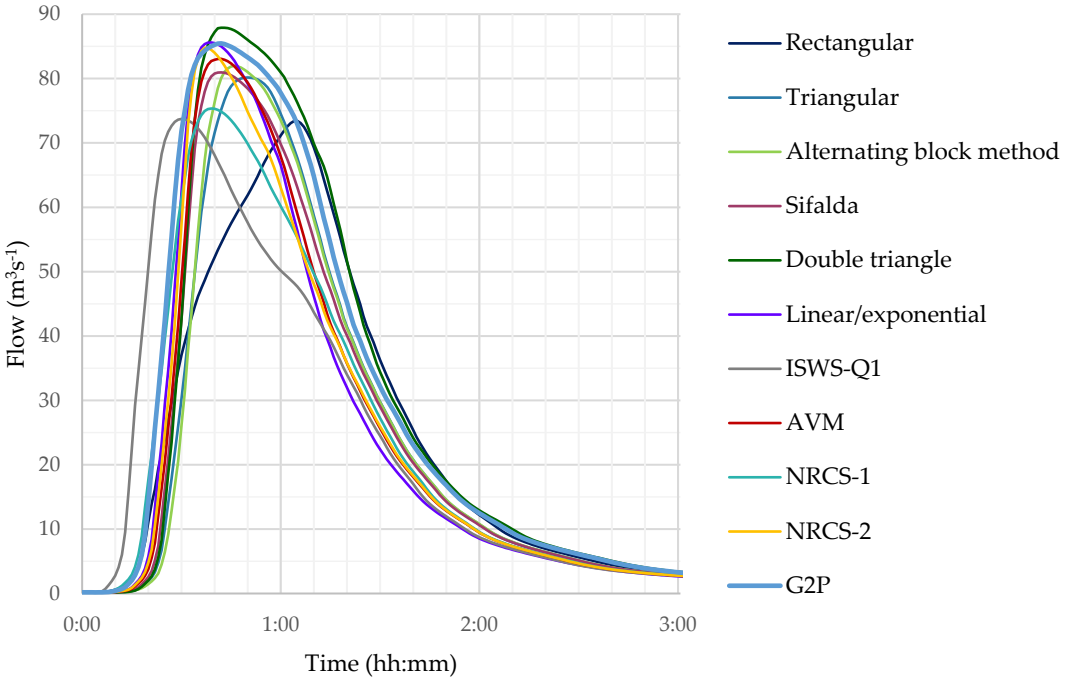

Figure 7. Hydrographs at the catchment outlet.

5. Discussion

The present research carried out a systematic comparison of several well-known design storms. All of them were obtained from the same rainfall series in Valencia, Spain, covering the period 1990 to 2012. For comparison purposes, all design storms were built with total duration of 1 hour, time level of aggregation of 10 min and return period of 25 years.

With the exception of the rectangular storm, the maximum rainfall intensities provided by Alternating Blocks, Sifalda, Linear/exponential, AVM and G2P storms are similar. In the case of the double triangle, ISWS-Q1 and NRCS-2 design storms, peak rainfall intensity is approximately 10% higher, whereas for the rest of the storms (triangular, NRCS-1) it is significantly lower (~25% lower).

The position of the maximum intensity is identical for most design storms, with the exception of ISWS-Q1, NRCS-1 and G2P, where the peak occurs earlier in time.

Concerning the temporal pattern, virtually all of them follow a typical pattern characterised by a rising limb of rainfall intensities, followed by the maximum and finally, a decreasing limb, which is somewhat longer. The only exceptions are the rectangular storm and the ISWS-Q1, in which the peak rainfall intensity appears earlier in time, i.e., in the first time interval.

The total cumulative rainfall derived from the different design storms is almost identical in all cases, except for the double triangle and the G2P ones, for which the cumulated volume is 14% higher.

On the basis of the former comparisons, it can be noticed that the four design storms presenting most common features are Alternating Blocks, Sifalda, Linear/exponential and AVM. In other words, these four design storms present very similar values in terms of total volume (mm), maximum intensity (mm h^{-1}), position of the maximum and temporal pattern. Hereon, we will refer to these storms as the standard design storms (SDS). The only (minor) discrepancy among these SDS is the position of the centroid, which is located slightly earlier in time for the Linear/exponential storm. It is worth noting the fact that, apart from AVM, the other three SDS are directly obtained from the IDF curve.

Regarding the peak discharges produced in the selected urban catchment, all SDS provide very similar values, with the exception of the Linear/Exponential one, which provides slightly higher discharge peaks (+5%).

Of course, the highest urban runoff discharges are produced by the design storms with highest volumes (mm) and peak intensities (mm h^{-1}). In particular, the double triangle design storm presents high values for both variables, leading to the highest maximum discharge (+8%), as should be expected. On the other hand, the G2P outstands due to its total cumulative rainfall depth, while the NRCS-2 yields to the highest peak intensity; both design storms are producing discharges which are slightly higher than the average (+5%).

In general, the discharges obtained with the rainfall–runoff model for the selected urban catchment, are reasonably similar for all SDS. Also the triangular, NRCS-2 and G2P storms produce estimated Q_p discharges that fall within the same range of values.

6. Conclusions

A selected family of 11 well-known design storms have been analysed and compared, attending to both the hyetographs themselves and the resulting hydrographs generated in a given real urban drainage system. Among them, there is a group consisting of a total of seven design storms (including the previously mentioned SDS), which essentially present very similar overall performance, attending to both the hyetographs and hydrographs. The remaining four design storms lead to hydrographs with more significant discrepancies:

a) Underaverage runoff: rectangular (−9%), ISWS-Q1 (−9%) and NRCS-1 (−7%).
b) Overaverage runoff: double triangle (+8%).

Focusing on the seven aforementioned design storms (the SDS group plus the triangular, NRCS-2 and G2P storms), only the AVM, NRCS-2 and the G2P consider the observed temporal pattern or historical storm occurrences in their construction procedure. Notwithstanding, it must be noted that only for AVM and G2P this aspect is incorporated through the direct analysis of the sample of

employed data (in this case, the series from the automatic rainfall gauge at Valencia). In the case of the NRCS-2 storm, the suggested temporal pattern does not come from the analysis of the Valencia data, as it is clear.

In agreement with the discussion presented herein, it is deemed advisable to employ the following design storms, depending on the availability of rainfall data.

In the case of design storms obtained from IDF curves, it is recommended to use the Alternating Blocks, Sifalda and Linear/exponential models. Among these three, the one that provides a more pessimistic result is the Linear/exponential one, since it provides a peak runoff discharge 5% higher than the other two for the analysed case.

The Sifalda design storm is remarkable for its easiness to build. Finally, the Alternating Blocks design storm presents the great advantage of being the most widely spread and internationally used referent; hence, it is the one which has been most extensively put in practice.

Among the design storms obtained directly from high-resolution historical data, the most recommendable ones are the AVM and the G2P. In this case, the G2P provides a runoff discharge which is slightly higher (+3%) than the one provided by the AVM. Both of them are built directly from the observed historical records, and thus share the advantage of preserving typical rainfall intensity patterns in statistical terms. The AVM method, widely employed in Australia since 1975, is a robust procedure that can be perfectly used in other climatic environments, as the present paper shows, providing good results. Concerning the more recent G2P synthetic storm, it should be pointed out that its practical application is generally somewhat more laborious, both in terms of parameter estimation and ulterior discretisation in temporal aggregation intervals. However, the essential advantage of the G2P when compared with the rest of design storms lies in its more compact analytical formulation, consisting of a single 2-parameter analytical function, as it is the case also of the Linear/exponential storm. In other words, the determination of two parameters is enough to ensure its complete definition. This property facilitates the systematic statistical treatment for regional analysis, allowing for future mapping of regional parameters for the characterisation of design storms to be used in urban hydrology cases.

Author Contributions: R.G.-B. and R.B.-S. reviewed the state-of–the-art; I.A.-D. processed the rainfall data; R.B.-S. compared the different design storms; I.A.-D. developed the urban drainage modelling application; R.G.-B. compared the different hydrographs; the three authors discussed the results, wrote and reviewed the paper.

Funding: This research received no external funding. The APC was funded by own funding from Universitat Politècnica de València.

Acknowledgments: The authors wish to acknowledge support from Confederación Hidrográfica del Júcar for providing the rainfall data used in this research and the City Council of Valencia for providing the case study for the urban drainage model applied.

Conflicts of Interest: The authors declare no conflicts of interest.

References

1. Wang, A.; Qu, N.; Chen, Y.; Li, Q.; Gu, S. A 60-Minute Design Rainstorm for the Urban Area of Yangpu District, Shanghai, China. *Water* **2018**, *10*, 312.
2. Schilling, W.; Fuchs, L. Errors in Stormwater Modeling—A Quantitative Assessment. *J. Hydraul. Eng.* **1986**, *112*, 111–123.
3. Viglione, A.; Blöschl, G. On the Role of Storm Duration in the Mapping of Rainfall to Flood Return Periods. *Hydrol. Earth Syst. Sci.* **2009**, *13*, 205–2016.
4. Adams, B.J.; Howard, C.D.D. Design Storm Pathology. *Can. Water Resour. J.* **1986**, *11*, 49–55.
5. Water Environment Federation; ASCE. *Design and Construction of Urban Stormwater Management Systems (Manual of Practice No.77)*; American Society of Civil Engineers: Los Angeles, CA, USA, 1992.
6. Larsen, T. Real Rainfall Time Series for Storm Sewer Design. In Proceeding of the Second International Conference on Urban Storm Drainage, Urbana, Illinois, USA, 15–19 June 1981; pp 358–364.
7. Willems, P. Stochastic Generation of Spatial Rainfall for Urban Drainage Areas. In *Water Science and Technology*; Elsevier: Amsterdam, The Netherlands, 1999.

8. Maßmann, S.; Krämer, S.; Fuchs, L.; Herrmann, O.; Kuchenbecker, A.; Birkholz, P.; Sympher, K.-J.; Haberlandt, U.; Morales, B.; Eisele, M.; et al. Applicability of Stochastically Generated Synthetic Rainfall Time Series for Urban Drainage Modelling. In *Geophysical Research Abstracts. EGU General Assembly*; 2019; Volume 21. Available online: https://meetingorganizer.copernicus.org/EGU2019/EGU2019-13776.pdf (accessed on 15 March 2019).
9. EN 752:2017. *Drain and Sewer Systems Outside Buildings. Sewer System Management.* Available online: https://www.thenbs.com/PublicationIndex/documents/details?Pub=NSAI&DocID=317478 (accessed on 26 February 2019)
10. Gong, Y.; Liang, X.; Li, X.; Li, J.; Fang, X.; Song, R. Influence of Rainfall Characteristics on Total Suspended Solids in Urban Runoff: A Case Study in Beijing, China. *Water* **2016**, *8*, 278.
11. Ahn, J.; Cho, W.; Kim, T.; Shin, H.; Heo, J.H. Flood Frequency Analysis for the Annual Peak Flows Simulated by an Event-Based Rainfall-Runoff Model in an Urban Drainage Basin. *Water (Switzerland)* **2014**, *6*, 3841–3863.
12. Marsalek, J.; Watt, W.E. Design Storms for Urban Drainage Design. *Can. J. Civ. Eng.* **1984**, *11*, 574–584.
13. Veneziano, D.; Villani, P. Best Linear Unbiased Design Hyetograph. *Water Resour. Res.* **1999**, *35*, 2725–2738.
14. Keifer, C.J.; Chu, H.H. Synthetic Storm Pattern for Drainage Design. *J. Hydraul. Div.* **1957**, *83*, 1–25.
15. Chow, V. Te; Maidment, D.R.; Mays, L.W. Applied Hydrology. McGraw-Hill, NY, USA, 1988.
16. Watt, W.E.; Chow, K.C.A.; Hogg, W.D.; Lathem, K.W. A 1-h Urban Design Storm for Canada. *Can. J. Civ. Eng.* **1986**, *13*, 293–300.
17. Pan, C.; Wang, X.; Liu, L.; Huang, H.; Wang, D. Improvement to the Huff Curve for Design Storms and Urban Flooding Simulations in Guangzhou, China. *Water (Switzerland)* **2017**, *9*, 1–18.
18. Kuichling, E. The Relation between the Rainfall and the Discharge of Sewers in Populous Districts. *Trans. Am. Soc. Civ. Eng.* **1889**, *20*, 1–56.
19. Yen, B.C.; Chow, V. Te. Design Hyetographs for Small Drainage Structures. *J. Hydraul. Div.* **1980**, *106*, 1055–1076.
20. Sifalda, V. Entwicklung eines Berechnungsregens für die Bemessung von Kanalnetzen. *gwf Wasser/Abwasser* **1973**, *114*, 435–440. (In German)
21. Desbordes, M. Urban Runoff and Design Storm Modelling. In *Proceedings of the International Conference on Urban Storm Drainage*; United Kingdom Pentech Press: London, UK, 1978; pp. 353–361.
22. Ellouze, M.; Abida, H.; Safi, R. A Triangular Model for the Generation of Synthetic Hyetographs. *Hydrol. Sci. J.* **2009**, *54*, 287–299.
23. Asquith, W.H.; Bumgarner, J.R.; Fahlquist, L.S. A Triangular Model of Dimensionless Runoff Producing Rainfall Hyetographs in Texas. *J. Am. Water Resour. Assoc.* **2003**, *39*, 911–921.
24. García-Bartual, R.; Andrés-Doménech, I. A Two Parameter Design Storm for Mediterranean Convective Rainfall. *Hydrol. Earth Syst. Sci.* **2017**, *21*, 2377–2387.
25. Lee, K.T.; Ho, J.-Y. Design Hyetograph for Typhoon Rainstorms in Taiwan. *J. Hydrol. Eng.* **2008**, *13*, 647–651.
26. Terstriep, M.L.; Stall, J.B. *The Illinois Urban Drainage Area Simulator, ILLUDAS*; Illinois State Water Survey: Urbana, IL, USA, 1974.
27. Cronshey, R. *Urban Hydrology for Small Watersheds*; US Dept. of Agriculture, Soil Conservation Service, Engineering Division: Washington, DC, USA, 1986.
28. Pilgrim, D.H.; Cordery, I. Rainfall Temporal Patterns for Design Floods. *J. Hydraul. Div.* **1975**, *101*, 81–95.
29. Peel, M.C.; Finlayson, B.L.; McMahon, T.A. Updated World Map of the Köppen-Geiger Climate Classification. *Hydrol. Earth Syst. Sci.* **2007**, *11*, 1633–1644.
30. Andrés-Doménech, I. Evaluación Probabilística de Indicadores de Eficiencia Para El Dimensionamiento Volumétrico de Tanques de Tormenta Para El Control de La Contaminación de Escorrentías Urbanas. Ph.D. Thesis, Universitat Politècnica de València, Valencia, Spain, 2010. (In Spanish)
31. Vaskova, I. Cálculo de Las Curvas IDF Mediante La Incorporación de Las Propiedades de Escala y de Dependencia Temporales. Ph.D. Thesis, Universitat Politècnica de València, Valencia, Spain, 2001. (In Spanish)
32. Sherman, C.W. Frequency and Intensity of Excessive Rainfalls at Boston, Massachusetts. *Trans. Am. Soc. Civ. Eng.* **1931**, *95*, 951–960.

33. Ajuntament de València (2016). Normativa para obras de saneamiento y drenaje urbano de la ciudad de Valencia. Ciclo Integral del Agua. Available online: https://www.ciclointegraldelagua.com/castellano/normativa-documentacion.php (accessed on 2 February 2019).
34. Barnolas, M.; Rigo, T.; Llasat, M.C. Characteristics of 2-D Convective Structures in Catalonia (NE Spain): An Analysis Using Radar Data and GIS. *Hydrol. Earth Syst. Sci.* **2010**, *14*, 129–139.
35. Rigo, T.; Llasat, M.C. A Methodology for the Classification of Convective Structures Using Meteorological Radar: Application to Heavy Rainfall Events on the Mediterranean Coast of the Iberian Peninsula. *Nat. Hazards Earth Syst. Sci.* **2004**, *4*, 59–68.
36. Water Pollution Control Federation. *Design and Construction of Sanitary and Storm Sewers (Manual of Practice no. 9)*; Water Pollution Control Federation, American Society of Civil Engineers: New York, NY, USA, 1969.
37. Huff, F.A. Time Distribution of Rainfall in Heavy Storms. *Water Resour. Res.* **1967**, *3*, 1007–1019.
38. Huff, F.A. *Time Distributions of Heavy Rainstorms in Illinois*; Illinois State Water Survey: Champaign, Circular. 173; 1990. Available online: http://hdl.handle.net/2142/94492 (accessed on 2 October 2017)
39. Andrés-Doménech, I.; García-Bartual, R.; Montanari, A.; Marco, J.B. Climate and Hydrological Variability: The Catchment Filtering Role. *Hydrol. Earth Syst. Sci.* **2015**, *19*, 379–387.
40. Alfieri, L.; Laio, F.; Claps, P. A Simulation Experiment for Optimal Design Hyetograph Selection. *Hydrol. Process.* **2008**, *22*, 813–820.
41. Cabo López, P. Caracterización Del Régimen de Descargas En El Sistema Unitario Del Colector Norte de Valencia. Master's Thesis, Universitat Politècnica de València, Valencia, Spain, 2017. (In Spanish)
42. Innovyze (2017). InfoWorks ICM Version: 8.5.0.17007 (64 bit). Available online: https://www.innovyze.com/en-us/products/infoworks-icm (accessed on 1 November 2017).
43. Preissmann, A. Propagation Des Intumescences Dans Les Canaux et Rivières, Paper Presented at 1st Congress of the French Association for Computation. In Proceedings of the First Congress of French Association for Computation, Grenoble, France, 14–16 September 1961.